APPLICATION OF ULTRASONIC SPECTROSCOPY TO SCATTERING OF RAYLEIGH WAVE IN A HALF-SPACE

Bien Q. Vu
Naval Ocean Systems Center
Code 9322
San Diego, CA 92152

Vikram K. Kinra
Aerospace Engineering Dept.
Texas A&M University
College Station, TX 77843

ABSTRACT

The scattering of Rayleigh surface waves by a variety of defects has been experimentally studied by the use of ultrasonic spectroscopy in the frequency range of 1 - 10 MHz. The defects are: (1) a through edge crack, both normal and inclined; (2) a cavity; (3) four different fluid inclusions, namely, carbon tetrachloride, water, mercury, and glycerine; (4) a solid inclusion; and (5) a shell. The transmission coefficient, A_T, defined as the total transmitted field normalized with respect to the incident field, is calculated from the FFT of the two signals. (The receiver is located sufficiently far away from the defect so that it only senses the far-field.) Whenever possible, the phase difference caused by the presence of the defect, ϕ, is also measured. The spectroscopic measurements were verified by the more accurate (albeit far more time consuming) tone-burst method. The classical problem of a quarter-space was used as a test case. The experimental results were found to be in excellent agreement with some of the recent analyses.

It is concluded that ultrasonic spectroscopy can be used as an efficient NDTE tool. In particular, the "signature" of a variety of inclusions is shown to be quite distinct, a fact that should prove very useful from the viewpoint of the inversion problem.

INTRODUCTION

The application of Rayleigh surface waves into the area of nondestructive testing and evaluation (NDTE) to estimate the size

of surface defects has been growing in recent years. One of the experimental techniques utilizes a broadband pulse (containing many frequencies) to obtain information about the defects from the frequency domain. This technique is called ultrasonic spectroscopy. The earliest application of ultrasonic spectroscopy is thickness measurement; the thickness is calculated from two consecutive spectral lines in the observed spectrum. The second application of ultrasonic spectroscopy is to examine the microstructure in material. By sending a broadband signal to the tested sample, the spectrum of the received signal yields information of grain size in the sample. For more information about the technique and its application, readers are referred to the review articles.[1,2]

Recently, many authors have applied the technique to more specific problems in NDTE. Sachse and his co-workers investigated the scattered field due to a cylindrical and spherical inclusion in an unbounded solid.[3] Morgan[4] examined the scattered field of a Rayleigh wave propagating toward the stepwise contour of a surface slot. Seydel and Frederick[5] used a P-wave to verify the location of three adjacent circular cylindrical cavities in an aluminum sample. Their results were correct to within 3% of the actual size.

In this work, ultrasonic spectroscopy has been used first to calculate the transmission and reflection coefficients of a Rayleigh wave propagating toward a quarter-space; later, to examine the spectral response of a cavity, a solid inclusion, a fluid inclusion and a shell.

EXPERIMENTAL PROCEDURES

In this work, the following types of imperfections were examined: (i) a line crack both normal and inclined to the free surface; (ii) a cavity; (iii) a tungsten inclusion, (iv) a tungsten shell; and (v) four different fluid inclusions, namely, carbon tetrachloride, water, mercury and glycerine. The half-space was modeled by a plate of aluminum 7075 whose acoustic properties were measured to be: longitudinal wavespeed C_1 = 6400 m/sec, shear wavespace C_2 = 3130 m/sec, attenuation α = 0.0023 nepers/mm and density ρ = 2.7 x 10^3 kg/m^3; Rayleigh wavespeed C_R = 2926 m/sec, acoustic impedances ρC_1 = 17.28 x 10^6 N-sec/m^3 and ρC_2 = 8.45 x 10^6 N-sec/m^3. The thickness of the plate was chosen to be 12.7 mm; the range of frequencies of the acoustic Rayleigh wave were chosen to be 1 - 10 MHz, which corresponds to the Rayleigh wavelengths 0.3 to 3 mm; therefore the state of plane strain can be assumed with ratio of the plate thickness to Rayleigh wavelength, B/λ_R = 4.5 to 45. The experimental justification of plane strain condition can be found in Ref. 8.

The edge crack was introduced to the aluminum plate by a diamond-impregnated wire saw, with the ratio of crack length to

crack width ℓ/d larger than 12, thus the crack can be safely assumed to be a line crack. The cavity and inclusion were introduced by drilling, reaming and lapping a through hole very close to the specimen surface. For the case of fluid inclusions, the fluid was poured into the cavity such that no air bubble is allowed to avoid the so-called "sloshing problem." The tungsten inclusion and shell were inserted into the cavity by the shrink-fit method to ensure a welded contact at the inclusion-matrix interface. In order to fill the possible microvoids at the inclusion-matrix interface, a low melting point compound , namely, phenyl salicylate (melting point = 43°C) was used to wet the hole wall prior to the inclusion insertion. An indirect, experimental technique to check the quality of the interface was presented in Ref. 8.

The transmitting and receiving transducers were coupled with the specimen by a polysterene wedge, whose acoustic properties were measured to be: longitudinal wavespeed C_w = 2340 m/sec, density ρ = 1.15 x 10^3 kg/m^3, thereby acoustic impedance ρC_w = 2.69 x 10^6 N-sec/m^3, attenuation α = 0.0035 neper/mm at 1 MHz and 0.0125 neper/mm at 5 MHz. The transducers are X-cut (compressional) crystals with center frequencies 1 MHz, 2 MHz, 5 MHz and 10 MHz. The wedge angle θ was calculated to be $\theta = \sin^{-1}(C_w/C_R) = 53°$ in order to generate Rayleigh waves along the specimen surface.

Near the imperfection, both the body waves and the Rayleigh waves are present, sufficiently far removed from the imperfection; however, the body waves attenuate either due to cylindrical expansion or due to mode conversion into the Rayleigh wave and, therefore, only a Rayleigh wave exists and it propagates without change. This is known as the scattered far field and the spectroscopic measurements were confined to the far field. Experience indicates that a distance of 10 λ_R from the scatterer was sufficient to guarantee far field.

A short duration spike of 20 nsec to 200 nsec was produced with the aid of a Sweep Generator (Wavetek Model 164). The pulse is amplified to an amplitude ranging from 50 to 300 volts and then applied to the transmitter. The received signal is displayed on an oscilloscope (Tek. 7704A), digitized and stored in the P-7001 Processor, and acquired in the Tek. 4051 computer. The Fourier spectra are then obtained by the use of standard FFT algorithms. The process is applied once to the specimen containing the imperfection, and again to the reference specimen (imperfection-free). The following information is gathered for each scatterer. Let $u_1(t)$ be the received signal for the specimen containing the imperfection; let $u_2(t)$ be the received signal for the reference specimen, i.e., the incident field; let $U_1(\omega)$, $\phi_1(\omega)$ and $U_2(\omega)$, $\phi_2(\omega)$ be, respectively, the amplitude and phase spectra of $u_1(t)$ and $u_2(t)$, then we define the reflection coefficient as $A_R(\omega) = |U_1(\omega)|/|U_2(\omega)$ when $u_1(t)$ is

the back-scattered field, and the transmission coefficient as $A_T(\omega) = |U_1(\omega)|/|U_2(\omega)|$ when $u_1(t)$ is the forward-scattered field. In either case, the phase shift is simply $\phi(\omega) = \phi_1(\omega) - \phi_2(\omega)$.

RESULTS AND DISCUSSION

In this section we report measurements concerning different types of imperfections. At first the results of the classical problem of a quarter-space were used as a test case. The comparison of this and the available results will be carried out. Then the case of the edge crack will be reported. Finally, the results of the cavity inclusion (solid and fluid) will be presented.

Transmission and Reflection Coefficients for a Quarter-Space

The quarter-space was chosen as a test case primarily for the reason that a number of research papers concerning it have been reported in the literature: experimental,[9-11] analytical,[12,13] as well as numerical.[14,15] Our experimental results were found to agree remarkably well with those reported in the literature.

The center frequencies of transducers used for this case were 1, 2, and 5 MHz. Since essentially the same results were obtained with all three transducers, in the following we report only the results obtained with the 2 MHz one. A_R and A_T were calculated from the amplitude spectra of the three pulses: the incident, the reflected and the transmitted ones. The results of the tone-burst measurements (points) and the ultrasonic spectroscopy measurements (solid lines) are compared in Fig. 1. Since the phenomenon is frequency-independent, the A_T and A_R curves were also averaged over the frequency range; these are shown as broken horizontal lines.

A compendium of the results available in the literature is presented in Table I; our results are also included for comparison. In particular, attention is drawn to recent analytical work by Achenbach, et al.,[12] who used ray theory to calculate A_R and A_T. Within the bounds of the experimental errors, our results agree extremely well with those of Ref. 12.

Case of an Edge Crack

The transmission and reflection coefficients A_T and A_R of a normal crack are presented in Fig. 2. The results from the ultrasonic spectroscopy are in solid lines and those from the tone-burst, triangles and squares. It may be seen in Fig. 2 that the spectroscopic data compared very well with the tone-burst data. The difference between the two is quite consistent with those expected from the error bounds: for A_R, the error in spectroscopy is ±5%; therefore the deviations between the two are expected to be ±20%. Note

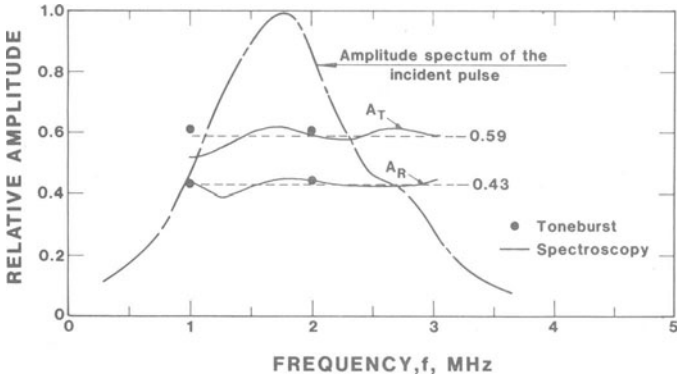

Fig. 1. A_T and A_R of a quarter-space, measured by spectroscopy using 2.25 MHz transducers (solid lines) and tone-burst (solid circles).

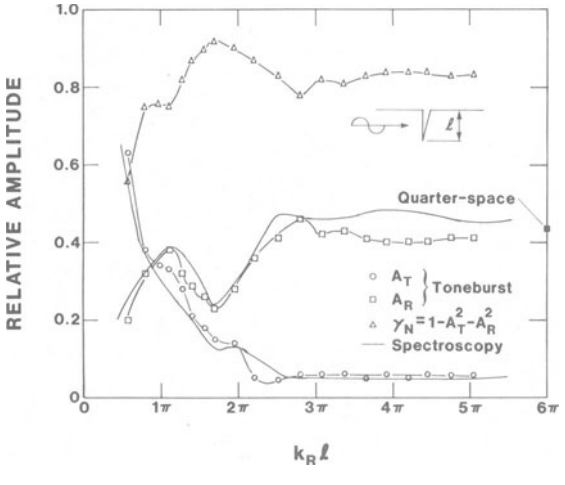

Fig. 2. A_T, A_R and γ_N for a normal edge crack. A comparison of tone-burst data and spectroscopic data (solid lines).

Table I

Transmission and Reflection Coefficients for a Quarter-Space

Sources	Poisson's Ratio	Refl. Coeff. A_R	Trans. Coeff. A_T	Scattered Energy $\gamma_N=1-A_T^2-A_R^2$
De Bremaecker [9] (Experimental, 1958)	0.17	0.38	0.63	0.46
Pilant et al. [10] (Experimental, 1964)	0.25	0.252	0.670	0.49
Munasinghe [15] (Numerical, 1973)	0.245	0.36	0.64	0.46
Bond [14] (Numerical, 1979)	0.24	0.43	0.57	0.49
Viktorov [11] (Experimental, 1962)	0.34	0.60	0.70	0.15
Cuozzo et al. [13] (Analytical, 1977)	0.33	0.38	0.75	0.29
Bond [14] (Experimental, 1979)	0.34	0.37	0.60	0.50
Bond [14] (Numerical, 1979)	0.34	0.47	0.59	0.43
Achenbach et al. [12] (Analytical, 1980)	0.33	0.40	0.60	0.48
This work (Tone-burst)	0.34	0.43	0.61	0.48
This work (Spectroscopy)	0.34	0.43	0.59	0.47

that the difference is always less than 20% and, in particular for $\ell/\lambda_R \leq 1.75$ it is less than 10%. For A_T, the error is ±10% in spectroscopy and ±5% in tone-burst, and therefore the discrepancy between the two is expected to be ±15%, which is borne out by the comparison in Fig. 2.

A_T and A_R of an inclined crack are presented in Fig. 3, from both spectroscopy and tone-burst techniques. The comparison is considered to be good and the discrepancy between the two sets of data is within the error bounds.

The remarkable results in Figs. 2 and 3 are the fairly well defined periodicity of equal interval on A_T, $2\ell/\lambda_R \simeq 1.0$ or $k_R\ell = \pi$. This periodicity is very clear in Fig. 3 and is seen to superimpose on an almost monotonic decrease of A_T with ℓ/λ_R. From the viewpoint of the inversion problem, the periodicity in itself is a sufficient and very accurate indicator of the crack length ℓ.

In conclusion, the spectroscopic data of the edge crack have been shown to be very useful for NDTE purposes.

Spectroscopic Analysis of a Tungsten Inclusion and a Cavity

In this section, we have examined the Fourier spectra (both the amplitude and the phase) for the case when a short duration (≃ 200 ns), broadband (0 - 10 MHz) Rayleigh pulse is scattered by a tungsten inclusion and a cavity of exactly the same radius and depth, namely, a = 0.51 mm and h = 0.78 mm; this yields $0 < ak_1 \leq 5$ and $0 < hk_2 \leq 15.7$. Only the forward total field was measured and the results are presented in the form of the transmission coefficients A_T. Figures 4a, b and c show, respectively, the time-domain data of the Rayleigh pulse received with the reference specimen (i.e., the incident pulse), with the specimen containing the cavity, and with the specimen containing the tungsten inclusion; Figs. 5 and 6 show the spectra for the cavity and the inclusion, respectively.

Attention is drawn to the time-domain data in Fig. 4. Note that the sweep rate (1 μsec/div.) and the vertical sensitivity (5 mV/div.) are kept identical in all three oscillographs. The time-delay (35.19 μsec.) between the excitation of the transmitter (t = 0) and the triggering of the oscilloscope is also kept the same. The following observations are made from Fig. 4:

1. The pulse received from the cavity is inverted (has a change of sign) relative to the incident pulse, suggesting thereby that a significant negative phase-shift is taking place.

2. The pulse shape for the tungsten inclusion is very similar to that of the incident pulse, suggesting that the phase change here

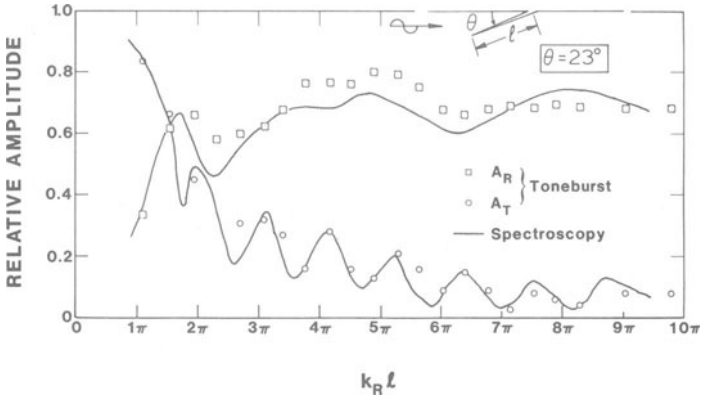

Fig. 3. A_T and A_R of an inclined crack, $\theta = 23^o$. A comparison of tone-burst data and spectroscopic data (solid lines).

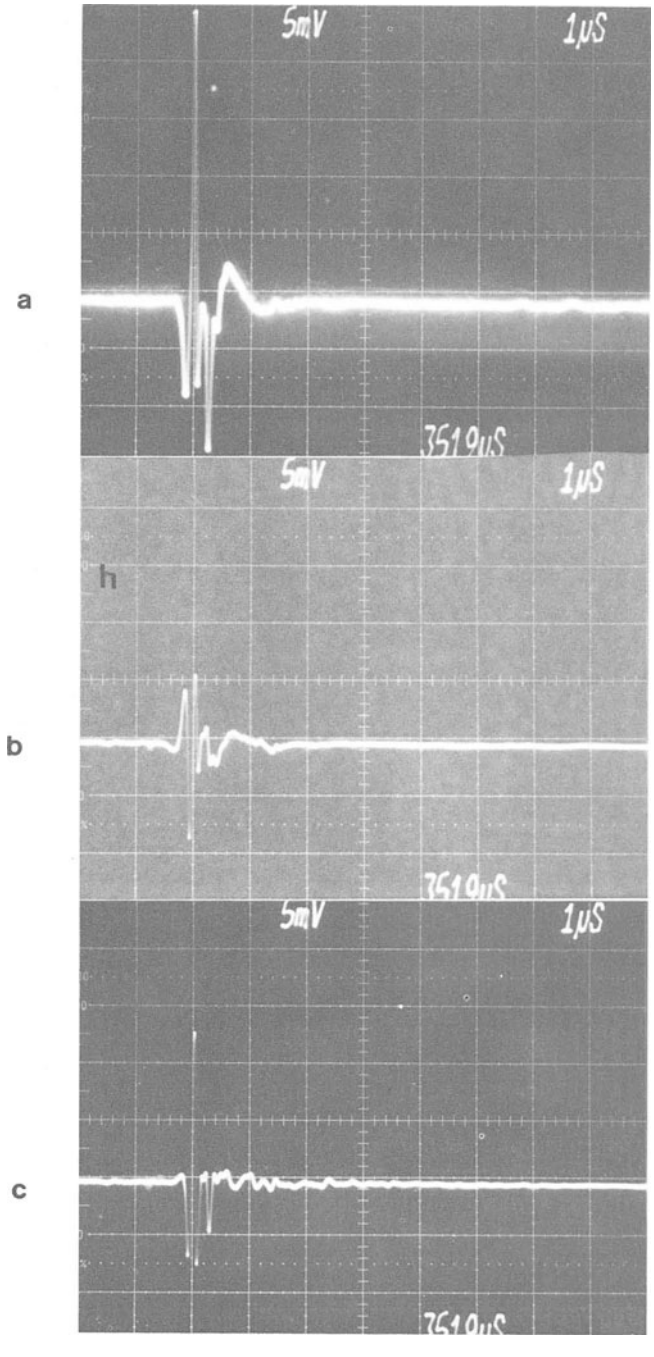

Fig. 4. Time-domain oscillographs of a broad band pulse: (a) Reference specimen; (b) cavity; and (c) tungsten inclusion.

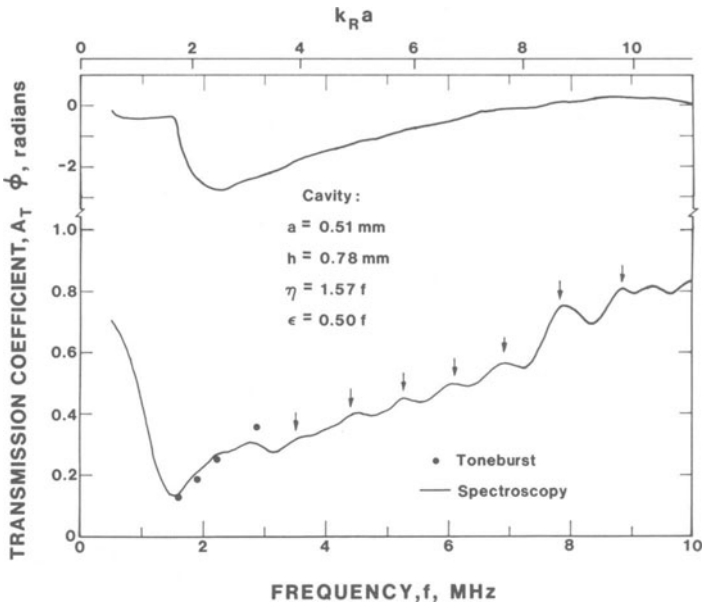

Fig. 5. Spectroscopic data for a cavity. a = 0.51 mm, h = 0.78 mm.

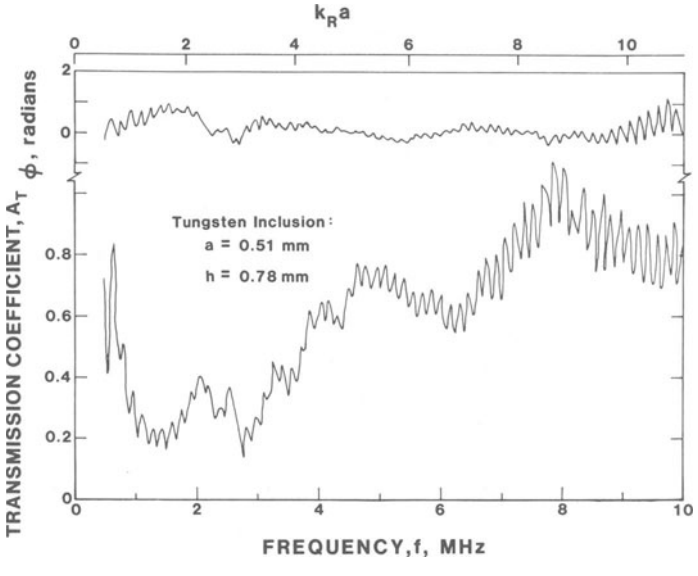

Fig. 6. Spectroscopic data of a tungsten inclusion. a = 0.51 mm, h = 0.78 mm.

is quite small. This is to be expected on physical grounds, for in the case of the cavity, most of the transmitted Rayleigh waves (except very low and high frequency components) must go around the cavity; the corresponding retardation time is about 0.2 μsec, which is too small to be detected in the time-domain data. On the other hand, as the Rayleigh wave transmits through the tungsten inclusion, since the wave velocities in tungsten and aluminum are very close to each other, the phase shift is expected to be small. For the case of a cavity, one can see the arrival of a discrete small pulse roughly 1.3 μsec after the first arrival; it is conjectured that this pulse is due to the Rayleigh wave which circumnavigates the cavity once; the calculated additional time is 1.10 μsec, which agrees fairly well with the observed time of 1.3 μsec. This phenomenon has been analyzed by Miklowitz[16] for the case of full-space. In the pulse from the tungsten inclusion, beyond the main signal, there is a multitude of ripples, which are probably due to the multiple reflections of the refracted waves within the inclusion and the surface-type waves circumnavigating the interface; however, the time-domain data do not lend to an easy interpretation.

It is readily seen from the above discussions that the time-domain data in Fig. 4 reveal very little information concerning the geometry and the elastic properties of the inclusion (or cavity). It is noted that Pao, Sachse and their co-workers[3,7,17] could extract useful information from the time-domain data, using ray theory, for the very much simpler geometry of a cavity/inclusion in a full-space, they used incident P-wave. In the following, we will examine the frequency-domain data which yield much more information about the inclusion and the cavity.

Cavity

Figure 5 shows the normalized amplitude spectrum, A_T, the phase shift relative to the incident pulse (labeled "phase"), and the amplitude spectrum of the reference signal. The connection between ε, η and the frequency, f, is also indicated. As expected, A_T reaches unity as $f \to 0$ (the wave does not "see" the cavity) and $f \to \infty$ (the penetration is less than ligament size). As f increases from 0.5 MHz, A_T decreases very radpily at first and attains a minimum at $f \simeq 1.6$ MHz ($\varepsilon = 0.80$, $\eta = 2.51$). Appropriate data from the tone-burst studies are shown as circles; note the satisfactory comparison. As f increases beyond 1.6 MHz, A_T exhibits a periodic structure with almost equal spacing between peaks and valleys; the mean value of this fluctuation is seen to increase monotonically with f. The peaks are indicated by the arrows. Miklowitz[16] has shown that when a plane compressional pulse in the shape of a Dirac delta function strikes a cavity in a full-space, circumferential waves are excited at the cavity surface and travel with the Rayleigh wave speed. Based on a simple kinematic argument, one would expect either the maxima or the minima of A_T to occur whenever the frequency

of the input signal increases by an amount which corresponds to the transit time, τ, of the Rayleigh wave once around the periphery, $\tau = 2\pi a/C_R = 1.10$ μs; thus if f_n and f_{n+1} are the frequencies at the two successive maxima (or minima), then $\Delta f = f_{n+1} - f_n = 1/\tau = 0.91$ MHz or $\Delta(k_R a) = 1$. The average spacing of the peaks in Fig. 5 is measured to be 0.88 MHz, which agrees remarkably well with the simple calculation given above. It is also noted that the periodic structure is very clear only within the range 3 MHz $\lesssim f \lesssim$ 9 MHz; it can be explained as follows. In the low frequency range, λ_R is large and the circumferential waves cannot exist; in the high frequency range, the penetration of the surface wave is too small to excite the circumferential waves in the first place.

Attention is now drawn to the phase (ϕ) curve in Fig. 5. Recall that this is the relative phase shift of $u^{(t)}$ with respect to $u^{(i)}$. ϕ is generally negative, which is consistent with the conjecture made earlier that the presence of the cavity delays the Rayleigh wave. Also $\phi \to 0$ as $f \to 0$ and $f \to \infty$ as expected. At first, ϕ shows a plateau to $f \simeq 1.6$ MHz and then has a sharp discontinuity there; it is very interesting to note that this discontinuity coincides with the minimum of A_T. Beyond this transition, ϕ increases monotonically to zero at 10 MHz.

Tungsten Inclusion

The Fourier spectra for the tungsten inclusion are shown in Fig. 6. If one temporarily ignores the ripples in the A_T curve, one notices a general similarity in the shape of the A_T curve for an inclusion and the cavity; in particular, the minimum at $f \simeq 1.6$ MHz. It would appear, therefore, that the source of this minimum is the same for both cases. As conjectured earlier, it is the excitation of a resonant mode when $1/f = 2\pi a/c$, where c is the phase velocity of the circumferential wave. The multitude of peaks is attributed to the doubly-infinite series of resonance frequencies of an elastic inclusion in an elastic full-space. (The resonance between the surface of the half-space and the inclusion does not affect these curves very much for the following reasons. The ligament $\ell = 0.27$ mm. For P-wave the first resonant frequency is 11.85 MHz, for S-wave it is 5.8 MHz.) Unfortunately, no analytical work addressing this problem could be found in the literature. However, with the assumption that such work will appear, an application of the A_T curve to NDTE is suggested. In any frequency range the number of peaks depends upon both the size and the elastic properties of the inclusion. Given the inclusion material, the size can be readily determined by simply counting the number of peaks. Conversely, if the size is known by some independent means (say metallography), the elastic properties can be readily found (application in materials science).

The phase curve also shows a definitely periodic structure; in fact, there appears to be a discontinuous phase-shift associated with each jump in A_T, i.e., with the (conjectured) excitation of a new resonance. Note that ϕ is rather small, which is consistent with the near-equality of wavespeeds of the two constituents.

Case of a Shell

The spectroscopic data obtained with a tungsten shell are presented in Fig. 7; the center-frequency of the transducers was 0.25 MHz. The interesting feature here is the existence of extrema points in all three quantities: A_T, A_R, and γ_N. This is probably due to excitation of resonant frequencies of the shell. This problem has been treated analytically by Datta, et al.;[18,19] however, direct comparison could not be made because of the vastly different value of t/a used in their numerical results. If, for the time being, one follows the simple kinematic argument that a resonance is set up when $k_R b$ = integer (b = outer radius of the shell), one obtains for the first resonance $k_1 a = 0.382$; the first peak in γ_N occurs at $k_1 a \simeq 0.4$ and the agreement is very good.

Case of a Fluid Inclusion

Four different fluids were tested: water, mercury, carbon tetrachloride and glycerine. The experiments revealed the existence of a very large number of resonant frequencies; these are compared with the predictions of a simple idealized model. Unfortunately, the comparison of the simple theory and the experiments was found not to be conclusive, in the following sense. A majority, but not all, of the experimentally observed peaks could be identified with the predicted ones; conversely, a majority, but not all, of the predicted peaks could be located in the data. Nevertheless, it is shown that this experimental approach has enormous potential usefulness in NDTE.

The description of all fluid inclusions is: a = 0.51 mm and h = 0.78 mm; in fact, this is the same physical specimen with which the air-filled (or empty) cavity results. The Fourier spectrum of the total received signal is shown in Fig. 8. The peaks in the spectra are due to the resonances of the fluid inclusion. Following the work of Mow and Workman[20] and Pao and Sachse[7] for the simpler case of a fluid inclusion in an unbounded rigid solid, the frequencies of the standing waves $f_{n,s}$ are calculated and tabulated in Table II. Here s = 1,2,3... as the overtones of the n^{th} mode. The modes with n = 0 represent axially symmetric vibrations of the inclusion. The first mode n = 1 has one nodal diameter, the second has two, and so on. The order of overtones indicates the number of nodal circles. Similar results are available for the other fluids examined.

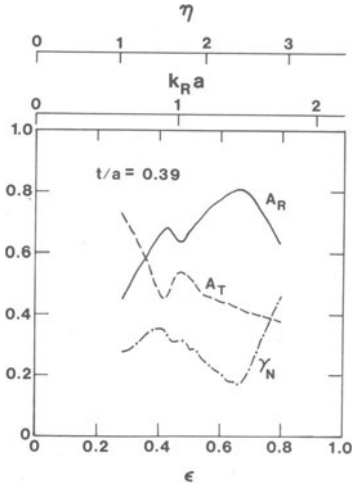

Fig. 7. Spectroscopic data of a tungsten shell. OD = 3.97 mm, ID = 2.67 mm, a = 1.66 mm, h = 3.43 mm (plane stress) in form of A_T, A_R and γ_N in the frequency range of 0.17 MHz to 0.48 MHz.

Comparison of the Theory and the Experiment

The resolution of the experiment, on the frequency scale, is 50 KHz (0.05 MHz). As is evident, we have a very large number of both the predicted and the observed resonant frequencies. Therefore an ad hoc criterion--that the observed and the calculated frequencies should agree to within 2 x 50 KHz = 100 KHz--was used to decide the correspondence between the theoretical and the experimental frequencies. These frequencies are indicated by down-pointing arrows in Fig. 8 and by asterisks in Table II. The modes of vibration and the overtones are also indicated.

With reference to Fig. 8 and Table II, the percentage of theoretically predicted peaks which could be identified experimentally are: 80% for water; 66% for mercury, 88% for carbon tetrachloride and 22% for glycerine. For the cases of water and carbon tetrachloride the comparison is considered very good. For the case of mercury

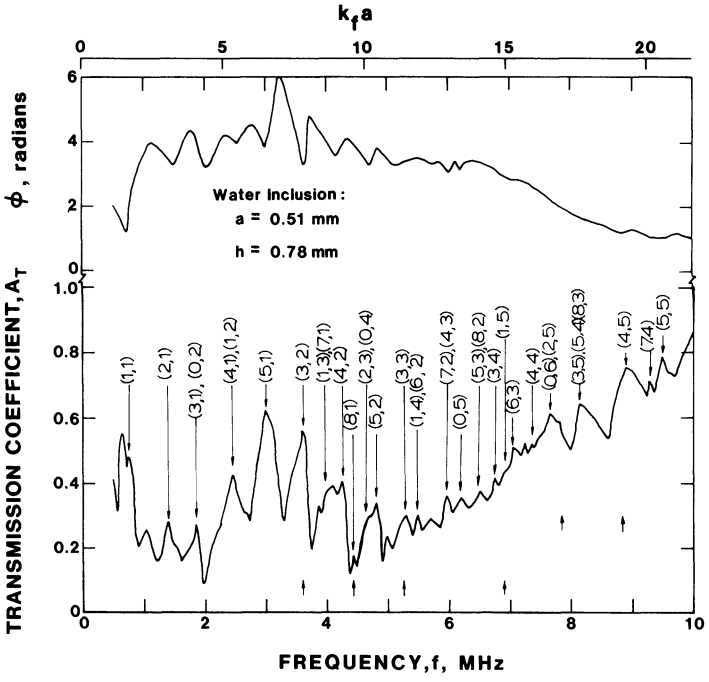

Fig. 8. Spectroscopic data of a water inclusion.
Upper: phase difference of $u^{(t)}$ with respect to $u^{(i)}$;
Lower: transmission coefficient A_T.

Table II

Natural Frequencies of a Water Inclusion,
$a = 0.51$ mm, $c_f = 1.483$ mm

s \ n	0	1	2	3	4	5	6	7	8
1	0	0.854	1.41*	1.95*	2.45*	2.97*	3.47	3.97*	4.46*
2	1.79*	2.48*	3.11	3.70*	4.29*	4.86*	5.42*	5.98*	6.53*
3	3.25	3.96*	4.64*	5.26*	5.86*	6.46*	7.01*	7.65*	8.23*
4	4.71*	5.42*	6.09	6.76*	7.39*	8.01*	8.62	9.23*	9.82
5	6.16*	6.88*	7.57*	8.22*	8.87*	9.52*	10.15		
6	7.62*	8.34	9.03	9.73	10.37				
7	9.08	9.79	10.49						
8	10.53								

* Frequencies which are excited in the experimental data.

the comparison is poor, most probably due to the following reason: the acoustic impedance of mercury and the aluminum matrix (for P-wave propagation) is very close, hence the assumption in the theory of the rigid boundary is clearly violated. This also explains why none of the resonant frequencies with n = 0 (axially symmetric motion) and only 3 with n = 1 are observed. (The resonant peak observed at 7.4 MHz is believed to be due to $f_{2,5} = 7.41$ MHz rather than $f_{0,6} = 7.46$ MHz.) Note that $f_{n,s}$, with large s are proportionately less sensitive to the violation of this assumption.

For the case of glycerine, the comparison is, once again, very poor. Here the reasons are altogether different. The theory assumes an inviscid fluid; glycerine is highly viscous. One would expect, therefore, that the resonance modes with a large n or s (i.e., large number of cells) will be damped out due to high velocity gradients.

Application of these Results in NDTE

When n is fixed and $s \gg n$, an approximate formula for evaluating the frequency difference of two overtones is

$$\Delta f_s = f_{n,s+1} - f_{n,s} \simeq C_f/2a \quad .$$

This empirical formula was used by Pao and Sachse[7] to obtain the approximate value of C_f of a fluid inclusion of known size. We now apply this empirical formula to our experimental results to the water inclusions. For water, we considered the following pairs of overtones: (0,4), (0,5); (0,5), (0,6); (1,2), (1,3); (1,3), (1,4); (1,4), (1,5); and (3,4), (3,5); the average value of C_f is calculated to be 1.499 mm/μsec compared to the correct value of 1.483 mm/μsec (1% discrepancy).

The above results from the empirical formula demonstrate a very promising prospect in NDTE. However, at this stage the application in NDTE is limited because for a fluid inclusion of unknown acoustic properties it is very difficult to identify the overtones of each particular mode of vibration from the spectroscopic data. More theoretical and experimental work is needed for the application of the above empirical formula in NDTE.

The transient response of a near-surface fluid inclusion to a broadband Rayleigh pulse has been examined in this section. Both the time-domain and the frequency-domain data contain information regarding the size and the acoustic properties of the constrained fluid. The potential application of these data in NDTE has been indicated.

CONCLUSIONS

It has been shown in this investigation that the technique of ultrasonic spectroscopy is a potential tool for NDTE.

ACKNOWLEDGEMENTS

The authors are grateful to Karl Rupp and Rich Cowgill, both from the Department of Mechanical Engineering, University of Colorado, Boulder, for their continued technical assistance through the course of this investigation. The financial aid of the National Science Foundation (Program Director, Clifford J. Astill) under Research Grant ENG 78-10168 and the Specialized Research Equipment Grant ENG 78-10869 is gratefully acknowledged.

REFERENCES

1. O.R. Gericke, "Ultrasonic Spectroscopy," Chapter 2 in Research Techniques in Nondestructive Testing, R.S. Sharpe (ed.), Academic Press, London, 1970.
2. L. Adler, K.V. Cook and W.A. Simpson, "Ultrasonic Frequency Analysis," Chapter 1 in Research Techniques in Nondestructive Testing, R.S. Sharpe (ed.), Academic Press, London, 1977.
3. W. Sachse and S. Golan, "The Scattering of Elastic Pulses and the Nondestructive Testing of Materials," Elastic Waves & Nondestructive Testing of Materials, AMD-29, ASME Winter Annual Meeting, Y.H. Pao (ed.), ASME, New York, 1978.

4. L.L. Morgan, "The Spectroscopic Determination of Surface Topography Using Acoustic Surface Waves," Acustica, Vol. 30, 222-228, 1979.
5. J.A. Seydel and J.R. Frederick, "A Computer-processed Ultrasonic Pulse-echo NDT System," Material Education, Vol. 31, 223-228, 1973.
6. D.A. Mendelsohn, J.D. Achenbach and L.M. Keer, "Scattering of Elastic Waves by a Surface-breaking Crack," Wave Motion, Vol. 2, 277-292, 1980.
7. Y.H. Pao and W. Sachse, "Interpretation of Time Records and Power Spectra of Scattered Ultrasonic Pulses in Solids," JASA, Vol. 56, 1478-1486, 1974.
8. B.Q. Vu and V.K. Kinra, "Diffraction of Rayleigh Waves in a Half-Space," CUMER Report 81-7, Dept. of Mechanical Engineering, University of Colorado, Boulder, CO, 80309, August 1981.
9. J.Cl. De Bremaecker, "Transmission and Reflection of Rayleigh Waves at Corners," Geophys., Vol. 23, 253-266, 1958.
10. W.L. Pilant, L. Knopoff and F. Schwab, "Transmission and Reflection of Surface Waves at a Corner, 3. Rayleigh Waves (Experimental)," J. Geophys. Res., Vol. 69, 291-297, 1964.
11. I.A. Viktorov, "Rayleigh Waves in Ultrasonic Range," Soviet Phys. Acoustic, Vol. 8, 119-129, 1962.
12. J.D. Achenbach, A.K. Gautesen and D.A. Mendelsohn, "Ray Analysis of Surface-Wave Interaction with an Edge Crack," IEEE Transaction on Sonics and Ultrasonics, Vol. SU-27, No. 3, 124-129, May 1980.
13. F.C. Cuozzo, E.L. Cambiaggio, J.P. Damiano and E. River, "Influence of Elastic Properties on Rayleigh Waves Scattering by Normal Discontinuity," IEEE Trans. Sonics and Ultraonics, Vol. SU-24, 280-298, 1977.
14. L.J. Bond, "A Computer Model of the Interaction of Acoustic Surface Waves with Discontinuities," Ultrasonics, Vol. 17, 71-77, 1979.
15. M. Munasinghe and G.W. Farnell, "Transmission and Reflection of Acoustic Surface Waves at Corners," Ultrasonics International, 250-255, 1973.
16. J.D. Miklowitz, "Scattering of a Plane Elastic Compressional Pulse by a Cylindrical Cavity," Proc. 11th Inter. Congress of Appl. Mech., Munich, Germany, H. Gortler, ed., Springer-Verlag, Berlin, 1964.
17. S. Sancar and W. Sachse, "Determination of the Geometry and Mechanical Properties of a Fluid-Filled Bi-Inclusion in an Elastic Solid," Ultrason. Symp. Proc., IEEE CAt. #76, CH 1120-5SU, 54-57, 1976.
18. N. El-Akily and S.K. Datta, "Response of a Circular Cylindrical Shell to Disturbances in a Half-Space," Earthquake Engr. and Struct. Dynamics, Vol. 8, 469-477, 1980.
19. S.K. Datta, A.H. Shah and N. El-Akily, "Dynamic Behavior of a Buried Pipe in a Seismic Environment," J. of Appl. Mechanics, Vol. 49, 141-148, 1982.
20. C.C. Mow and J.W. Workman, "Dynamic Stresses around a Fluid-Filled Cavity, J. of Appl. Mechanics, Vol. 33, 793-799, 1966.